Annals of Botany **XX**: 1–13, 2019
doi: 10.1093/aob/mcz025, available online at www.academic.oup.com/aob

ANNALS OF BOTANY
Founded 1887

Leaf heteroblasty in *Passiflora edulis* as revealed by metabolic profiling and expression analyses of the microRNAs miR156 and miR172

Priscila O. Silva[1], Diego S. Batista[1,2], João Henrique F. Cavalcanti[3,4], Andréa D. Koehler[1], Lorena M. Vieira[1], Amanda M. Fernandes[1], Carlos Hernan Barrera-Rojas[5,6], Dimas M. Ribeiro[2], Fabio T. S. Nogueira[5,*] and Wagner C. Otoni[1]

[1]Departamento de Biologia Vegetal/Instituto de Biotecnologia Aplicada a Agropecuária (BIOAGRO), Universidade Federal de Viçosa, 36570–900, Viçosa, Minas Gerais, Brazil, [2]Universidade Estadual do Maranhão, 65055–310, São Luís, MA, Brazil, [3]Departamento de Biologia Vegetal, Universidade Federal de Viçosa, 36570–900, Viçosa, Minas Gerais, Brazil, [4]Instituto de Educação, Agricultura e Ambiente, Universidade Federal do Amazonas, 69800-000, Humaitá, Amazonas, Brazil, [5]Escola Superior de Agricultura Luiz de Queiroz, Universidade de São Paulo, 13418–900, Piracicaba, São Paulo, Brazil and [6]Instituto de Biociências, Universidade Estadual de São Paulo, 18618–970, Botucatu, São Paulo, Brazil
**For correspondence. E-mail: ftsnogue@usp.br*

Received: 19 November 2018 Returned for revision: 15 January 2019 Editorial decision: 4 February 2019 Accepted: 7 February 2019

• **Background and Aims:** Juvenile-to-adult phase transition is marked by changes in leaf morphology, mostly due to the temporal development of the shoot apical meristem, a phenomenon known as heteroblasty. Sugars and microRNA-controlled modules are components of the heteroblastic process in *Arabidopsis thaliana* leaves. However, our understanding about their roles during phase-changing in other species, such as *Passiflora edulis*, remains limited. Unlike *Arabidopsis*, *P. edulis* (a semi-woody perennial climbing vine) undergoes remarkable changes in leaf morphology throughout juvenile-to-adult transition. Nonetheless, the underlying molecular mechanisms are unknown.
• **Methods:** Here we evaluated the molecular mechanisms underlying the heteroblastic process by analysing the temporal expression of microRNAs and targets in leaves as well as the leaf metabolome during *P. edulis* development.
• **Key Results:** Metabolic profiling revealed a unique composition of metabolites associated with leaf heteroblasty. Increasing levels of glucose and α-trehalose were observed during juvenile-to-adult phase transition. Accumulation of microRNA156 (miR156) correlated with juvenile leaf traits, whilst miR172 transcript accumulation was associated with leaf adult traits. Importantly, glucose may mediate adult leaf characteristics during *de novo* shoot organogenesis by modulating miR156-targeted *PeSPL9* expression levels at early stages of shoot development.
• **Conclusions:** Altogether, our results suggest that specific sugars may act as co-regulators, along with two microRNAs, leading to leaf morphological modifications throughout juvenile-to-adult phase transition in *P. edulis.*

Key words: Heteroblasty, microRNA, sugar, *de novo* shoot organogenesis, *Passiflora edulis*.

INTRODUCTION

Plants undergo successive development stages during their life cycle, adopting different genetic and molecular mechanisms that provide them with alternatives to express their plasticity and, consequently, to adjust themselves morpho-physiologically to distinct environments (Yu *et al.*, 2015; Fouracre and Poethig, 2016). In some species, the transition from juvenile to adult phase is marked by evident changes in leaf morphology and by the acquisition of reproductive competence mediated by physiological, genetic and molecular responses (Poethig, 2010; Huijser and Schmid, 2011).

Heteroblasty is one of the most intriguing mechanisms that contribute to leaf shape diversification, both within a single plant and between species. Heteroblasty is generally described as the temporal development of the shoot apical meristem, which potentially affects several traits of the lateral organs, including their morphology. Considerable progress has been made in characterizing the genetic and molecular mechanisms underlying the heteroblastic process (Wang *et al.*, 2009; Tsukaya, 2013; Yu *et al.*, 2013). Compelling evidence demonstrates that microRNAs, together with transcription factors and phytohormones, integrate a complex regulatory network that plays key roles in plant vegetative development (Mallory and Vaucheret, 2006; Liu and Chen, 2009). MicroRNAs are a class of small endogenous non-coding RNAs (20–22 nucleotides) that regulate gene expression mostly at post-transcriptional levels through RNA–RNA interactions in both animals and plants (Lagos-Quintana *et al.*, 2001; Jones-Rhoades *et al.*, 2006; Khraiwesh *et al.*, 2010; Axtell *et al.*, 2011). Among the microRNAs involved in the regulation of vegetative phase change, the ancient and highly conserved microRNA156 (miR156) (Morea-Ortiz *et al.*, 2016) is essential for the maintenance of the juvenile phase. MiR156 and targets [transcription factors belonging to the SQUAMOSA PROMOTER-BINDING

PROTEIN-LIKE (SPL) family] define an age-dependent pathway along with the miR172-regulated module that controls leaf morphological changes during the juvenile-to-adult transition and flowering time in several species (Wang *et al*., 2009, 2011; Wu *et al.*, 2009; Chen *et al.*, 2010; Levy *et al.*, 2014; Silva *et al.*, 2019). Previous studies have shown that miR156 is highly expressed at early stages of shoot development and its expression levels decrease as the plant ages. On the other hand, *SPL* genes and miR172 exhibit an opposite expression pattern (Wu *et al.*, 2009; Yu *et al.*, 2015; Nguyen *et al.*, 2017).

The gradual decline in miR156 levels during the juvenile-to-adult transition allows the expression of adult characteristics in leaves. However, the mechanisms by which the levels of this microRNA are regulated throughout leaf development are not fully understood (Yu *et al.*, 2015). Recent work has revealed that the miR156–*SPL* module is subjected to epigenetic regulation during juvenile-to-adult transition, such as DNA methylation, histone modifications and chromatin remodelling (M. Xu *et al.*, 2018; Y. Xu *et al.*, 2018). Furthermore, two components of the Mediator CDK8 module [CITY (CCT) and GRAND CENTER (GCT)] were shown to regulate the amplitude of miR156 expression during vegetative phase transition in *Arabidopsis thaliana* (Gillmor *et al.*, 2014). However, little is known about possible metabolites that regulate or act in parallel to this microRNA-controlled module during leaf development. Although the importance of metabolites in the juvenile-to-adult vegetative phase change was highlighted decades ago by Corbesier *et al.* (1998), only recently have studies described sugar as one of the possible metabolites involved in *Arabidopsis* vegetative development via the modulation of the miR156–*SPL* module (Yu *et al.*, 2013; Smeekens *et al.*, 2010). Low levels of miR156 and increasing sugar content were associated with the acquisition of adult traits in *Arabidopsis* leaves (Yang *et al.*, 2013; Yu *et al.*, 2013). Accordingly, the *Arabidopsis cao/chlorina1* (*ch1*) mutant, with reduced photosynthesis, shows a delay in vegetative phase change, highlighting the involvement of sugars and photoassimilates in modulating heteroblastic traits in leaves (Yang *et al*., 2011, 2013; Yu *et al.*, 2013).

During vegetative development, the phenotypic expression of the heteroblastic progress of leaves changes according to the species and responds to fluctuations in the environmental conditions (Gamage, 2011; Chitwood *et al.*, 2014). Although the genetic and molecular mechanisms involved in the heteroblastic process appear to be largely conserved (Yu *et al.*, 2015), the majority of studies involving genetic pathways regulated by microRNAs and metabolites have focused on model plants. For instance, studies on the morphological and molecular bases that control leaf shape and juvenile-to-adult phase change are mostly concentrated in species such as *Arabidopsis*, *Oryza sativa* and *Zea mays* (Chuck *et al.*, 2007; Yu *et al.*, 2013; Wang *et al.*, 2015; Xu *et al.*, 2016).

Passiflora edulis is one of the 500 species belonging to the genus *Passiflora* and a tropical fruit crop known as passion fruit (De Wilde, 1971; Cronquist, 1988). *Passiflora edulis* is a semi-woody perennial climbing vine that produces large attractive flowers. Importantly, *P. edulis* displays extreme changes in leaf morphology between juvenile and adult phases, and it has been recently proposed as a new model for investigating different developmental processes, including flowering and leaf heteroblasty (Nave *et al.*, 2010; Chitwood and Otoni, 2017*a*, *b*). At the beginning of vegetative development in *P. edulis*, the young leaves are monolobed and lanceolate-shaped, with small leaf blades and smooth margins. As the vegetative-to-adult transition progresses, the leaves experience complex morphological modifications, displaying larger leaf blades, serrated margins and the formation of new lobes, going from monolobed to trilobed (Cutri *et al.*, 2013; Chitwood and Otoni, 2017*a*, *b*). Importantly, changes in shape and size occur gradually throughout leaf development, which suggests that *P. edulis* may become a promising model for evaluating genetic and molecular mechanisms underlying juvenile-to-adult vegetative phase transition in leaves. However, there is no report on regulatory networks associated with vegetative phase change in *P. edulis*, especially those including microRNAs and metabolites.

In this study, we investigated the temporal expression patterns of miR156 and one of its targets (*P. edulis SPL9* or *PeSPL9*), as well as miR172, during the heteroblastic process in *P. edulis* leaves. We show that high levels of miR156 were associated with juvenile traits and that its expression declined in leaves even before obvious morphological changes were noticed. On the other hand, high miR172 expression levels were observed in leaves displaying adult traits. We also monitored the hormone and metabolic profiles of leaves during the vegetative-to-adult transition. Levels of cytokinin and auxin were higher as early as the sixth leaf. Increasing levels of soluble sugars, including glucose, were associated with adult traits. Moreover, supplementation of the culture medium with glucose induced adult leaf characteristics during *de novo* shoot organogenesis, with subsequent accumulation of *PeSPL9* transcripts. We discuss the potential role of soluble carbohydrates acting along with microRNAs during the heteroblastic process in *P. edulis* leaves.

MATERIALS AND METHODS

Plant material and growth conditions

Seeds of *Passiflora edulis*, population FB300, provided by Viveiros Flora Brasil Ltda (Araguari, MG, Brazil) were sown and germinated in trays. Subsequently, 40-d-old *P. edulis* seedlings were transferred and grown in 5-L plastic pots containing commercial substrate [Tropstrato HT Hortaliças® (vermiculite, mixture 14:16:18, potassium nitrate, simple and superphosphate; Vida Verde Indústria e Comércio Ltda, Mogi Mirim, SP, Brazil)]. Plants were grown in greenhouse conditions under a photoperiod of 12/12 h (day/night), 25/16 °C (day/night). The third, sixth, ninth, tenth, eleventh and twelfth fully expanded leaves, from the base to the apex, were collected after 30 d post-emergence (dpe) of a leaf primordium. To further compare the metabolic profile of younger leaves with 30-dpe leaves by using principal component analysis (PCA; see Statistical analysis section), we additionally harvested *P. edulis* leaves at 15 dpe as described above. Leaf samples were collected in liquid nitrogen and stored at −80 ºC until used for biochemical, metabolic and molecular analyses.

Leaf growth dynamics

The growth in width and length of the third, sixth, ninth, tenth, eleventh and twelfth leaves of *P. edulis* was evaluated

every 3 d over a 30-d period after emergence of a leaf primordium. Leaf growth was described by the sigmoidal function.

Hormone quantification

Approximately 100 mg of fresh *P. edulis* leaf tissue was macerated in liquid nitrogen followed by the addition of 300 µL of extractive solution (methanol:isopropanol:acetic acid 20:79:1). Subsequently, the samples were vortexed (four times for 20 s), sonicated (5 min) and maintained on ice (30 min). After centrifugation (13 000 *g*, 10 min at 4 °C), 250 µL of the supernatant was collected into a new tube. The extraction procedure was repeated on the resulting pellet, and the supernatants were collected. The Agilent 6430 Triple Quadrupole LC/MS system (Agilent Technologies, Waldbronn, Germany) was used for identification and quantification, according to Napoleão *et al.* (2017).

RNA extraction and stem–loop pulsed RT–qPCR

Total RNA was isolated using TRI-Reagent® solution (Sigma-Aldrich, St Louis, MO, USA) and treated with DNAse I (Thermo Scientific, Wilmington, DE, USA). DNase I-treated RNA (1 µg) was reverse-transcribed to generate first-strand cDNA, as described previously (Varkonyi-Gasic *et al.*, 2007). PCR reactions were performed using SYBR Green Mix/Rox (Ludwig Biotec®, Alvorada, Brazil) and analysed in a StepOnePlus real-time PCR system (Applied Biosystems). Two or three biological samples with three technical replicates each were used in the RT–qPCR analyses. Expression levels were calculated relative to the housekeeping gene *PeACTIN1* (Cutri and Dornelas, 2012) using the ΔΔct method (Livak and Schmittgen, 2001). The primers used are listed in the Supplementary Data Table S1.

Sugar content determination

Leaf samples were collected at the end of the day (1 h before dark) and subjected to ethanol extraction. In the soluble fraction, glucose, fructose and sucrose contents were determined according to the methodology described by Fernie *et al.* (2001). To estimate sugar concentration (results expressed in µmol g^{-1}), an equation based on the Lambert–Beer law was applied: µmol NADPH = ΔOD/(2.85 × 6.22).

Metabolic profile

Leaf samples were extracted in methanol, water and chloroform, with ribitol as the internal standard (0.2 mg mL^{-1}) as previously described (Lisec *et al.*, 2006). After extraction, the upper polar phase containing the primary polar metabolites was collected and dehydrated in a SpeedVac (Concentrator plus, Eppendorf). These samples were derivatized by adding 40 µL of methoxyamine hydrochloride (20 mg mL^{-1} in pyridine) and incubating for 2 h at 37 °C with shaking at 950 *g* (Thermomixer comfort, Eppendorf). Next, 70 µL of solution containing 1 mL of *N*-methyl-*N*-(trimethylsilyl) trifluoroacetamide and 20 µL of fatty acid methyl esters (FAME) was added and incubation was continued for 30 min at 37 °C, with agitation at 950 *g*. A volume of 100 µL was transferred to vials and used to determine the metabolic profile by gas chromatography coupled with mass spectrometry (GC–MS TruTOF System, Agilent-LECO) (Roessner *et al.*, 2001). Chromatograms and mass spectra were evaluated using the software Chroma TOF 4.4 (LECO) and TargetSearch (Luedemann *et al.*, 2008) fed with a library containing the retention times and fragmentation pattern of the primary metabolites of the Golm Metabolom database. Once identified, the data were normalized with the internal standard ribitol and are presented as values relative to the values for the third leaf. This analysis allowed the determination of the main classes of compounds (amino acids, organic acids, sugars and others).

Effect of glucose on modulation of leaf morphology during the in vitro *heteroblastic process*

Thirty-day-old seedlings were grown on half-strength Murashige and Skoog (MS)-based medium (Murashige and Skoog, 1962) according to Reis *et al* (2003) and used as a source of cotyledonary explants. Cotyledons were cut into small fragments (average 6 mm^2) and placed in glass flasks (250 mL capacity) containing 50 mL of MS medium supplemented with B5 vitamins (Gamborg *et al.*, 1968), 100 mg L^{-1} myo-inositol, 2.5 g L^{-1} (Phytagel®, Sigma, USA), pH 5.8. To induce adult leaf morphological traits *in vitro*, the explants were cultured in induction medium (IM) containing MS-based culture medium at half of the hormone concentration [MS medium supplemented with 10 µM benzyladenine, 5 µM kinetin and 2.5 µM indole-3-acetic acid (IAA)], as suggested by Drew (1991). The explants were cultured as follows: (1) incubation in IM without glucose; (2) incubation in IM supplemented with 44 mM glucose; or (3) incubation in IM supplemented with 88 mM glucose.

Isolation and sequencing of P. edulis SPL9 *gene expressed during leaf development*

To amplify the *Arabidopsis* miR156-targeted *SPL9* homologue in *P. edulis*, first-strand cDNA was synthesized from 3.0 µg of total RNA isolated from a pool of leaves in different developmental stages. Degenerate primers (Supplementary Data Table S1) were designed from conserved regions of the *Arabidopsis SPL9* mRNA sequence (https://www.arabidopsis.org/). PCR reactions were performed using Platinum Taq DNA Polymerase High Fidelity® (Thermo Fisher Scientific). The 5′ and 3′ cDNA ends were complemented by RACE (rapid amplification of cDNA ends) reactions, using as template an adaptor-ligated double-stranded cDNA library, previously obtained through poly(A)+RNA isolated using Marathon® cDNA Amplification (Clontech), according to the manufacturer's recommendations. PCR reactions were performed using Taq DNA Polymerase Advantage® (Clontech). The amplification

product was ligated into the plasmid pGEM®-T Easy Vector Systems (Promega®) and introduced into ultracompetent cells of *Escherichia coli* (DH5α strain). Positive clones were sequenced with forward and reverse M13 universal primers (Macrogen Company, South Korea).

After sequence analysis, a putative contig was generated and submitted to BLAST analysis (Altschul *et al.*, 1997). For identification of conserved domains, the conserved domain database database was used (http://www.ncbi.nlm.nih.gov/Structure/cdd/cdd.shtml). Alignment of the protein sequence was generated by the Bioedit v7.0.5 Software. The *SPL9* open reading frame was identified by ORFfinder. A similarity tree with SPL9 proteins from other species was estimated by the neighbour-joining method (Saitou and Nei, 1987) using MEGA Software, version 7.0 (Kumar *et al.*, 2014). Subsequently, *SPL9*-pecific primers were designed to monitor the expression levels of *PeSPL9* (Supplementary Data Table S1).

Localization of PeSPL9 *transcripts by* in situ *hybridization*

De novo regenerated shoots were fixed in 4 % paraformaldehyde for 16 h. The samples were dehydrated in an ethanol series and gradually embedded in Histosec® paraffin (Merck Millipore, Germany). Sections (4 µm) were obtained and placed on Fisherbrand Probe One Plus™ Microscope Slides (Fisher Scientific, USA). Antisense and sense RNA probes labelled with digoxigenin (DIG–UTP) contained part of the C-terminal and the 3′-UTR of the gene. The probes were synthesized by *in vitro* transcription using the DIG RNA Labeling Kit (SP6/T0) according to the manufacturer's recommendations (Roche Applied Science). All steps in the hybridization reaction, washes and immunological detection were performed according to Rocha *et al.* (2018). Images were analysed under an optical microscope (AX70 TRF, Olympus Optical) with the U-Photo System coupled to a digital system (Spot Insightcolour 3.2.0, Diagnostic Instruments).

Statistical analyses

For soluble sugar quantification and metabolic profiling of *P. edulis* leaves, the experimental unit consisted of five biological replicates, composed of a three-leaf pool. For the morphogenic parameters, six replicates were used, each consisting of one flask containing ten explants. Analysis of variance ($P < 0.05$) was carried out to determine effects of the treatments. Differences were evaluated by the Scott–Knott test (Scott and Knott, 1974) at the 5.0 % significance level. For gene expression analysis, the Mann–Whitney test at the 5.0 % significance level was applied.

To investigate the changes in metabolites associated with leaf heteroblasty in distinct developmental stages (15- and 30-dpe leaves), PCA (Krumsiek *et al.*, 2016) including all metabolite data was employed using Minitab software.

RESULTS

Leaf growth dynamics and morphological changes

Heteroblasty, the temporal development of the meristem, can produce diverse leaf shapes within a plant. As expected, the heteroblastic pattern of *P. edulis* leaves was altered during juvenile–adult vegetative development (Fig. 1). In early stages of vegetative development, young leaves were monolobed with a lanceolate-like shape, small leaf blade and smooth margins. As vegetative development progressed, the transition from juvenile to adult phase was marked by an intermediate phase, when both young and adult traits were observed on the same leaf (eighth and ninth leaves; Fig. 1A). During the course of vegetative maturation the leaf became more complex, with a larger leaf blade, serrated margins and the formation of new lobes. From the tenth leaf onwards, heteroblastic growth became apparent as the morphological pattern switched from monolobed to trilobed (Fig. 1A). This heteroblastic behaviour is observed in several species of the genus *Passiflora* (Chitwood and Otoni, 2017*a*, *b*). The growth dynamics of the third, sixth, ninth, tenth, eleventh and twelfth leaves at 30 dpe conformed to a sigmoidal function (Fig. 1B, C). Young and adult leaves showed similar growth patterns in both length and width throughout the heteroblastic process. Leaf growth (both in length and width) occurred exponentially until ~15 dpe. After this time, growth rate was limited, suggesting that *P. edulis* leaves cease growing around 30 dpe (Fig. 1B, C). Thus, to avoid comparing leaves at different emergence stages, we decided to evaluate the heteroblastic process in young to adult 30-dpe leaves.

Hormones levels dynamically change during the heteroblastic process in P. edulis *leaves*

Auxin homeostasis and jasmonic acid signalling have been associated with leaf development (Ostria-Gallardo *et al.*, 2016; Huang *et al.*, 2017). Therefore, we investigated the fluctuations in hormone levels during the progression of the heteroblastic process in 30-dpe *P. edulis* leaves by measuring endogenous auxin (IAA), methyl jasmonate (MeJa), zeatin and 1-amino-cyclopropane-1-carboxylic acid (ACC) levels, using LC–MS. Zeatin, IAA and ACC levels increased already in the sixth leaf (Fig. 2A–C). While the amounts of ACC (which reflects endogenous levels of ethylene) and zeatin did not differ significantly during the heteroblastic process, the IAA level showed its peak in the 12th leaf. These results show that IAA accumulation was correlated with the appearance of adult traits and the formation of leaf lobes in 30-dpe *P. edulis* (Fig. 2B), and they are consistent with recent data from other species suggesting that the modulation of auxin biosynthesis is associated with heteroblasty (Ostria-Gallardo *et al.*, 2016). On the other hand, our results showed higher levels of MeJa in young leaves followed by a moderate reduction in adult leaves (Fig. 2D). Taken together, our data suggest a temporal balance of hormone levels during the heteroblastic process of *P. edulis* leaves.

Variation in the levels of soluble carbohydrates and distinct metabolites correlates with juvenile-to-adult vegetative transition

For decades, there have been indications that sugars are important for shoot maturation, not only because of their classical functions in metabolism but also because sugars can act as signalling molecules in several developmental processes,

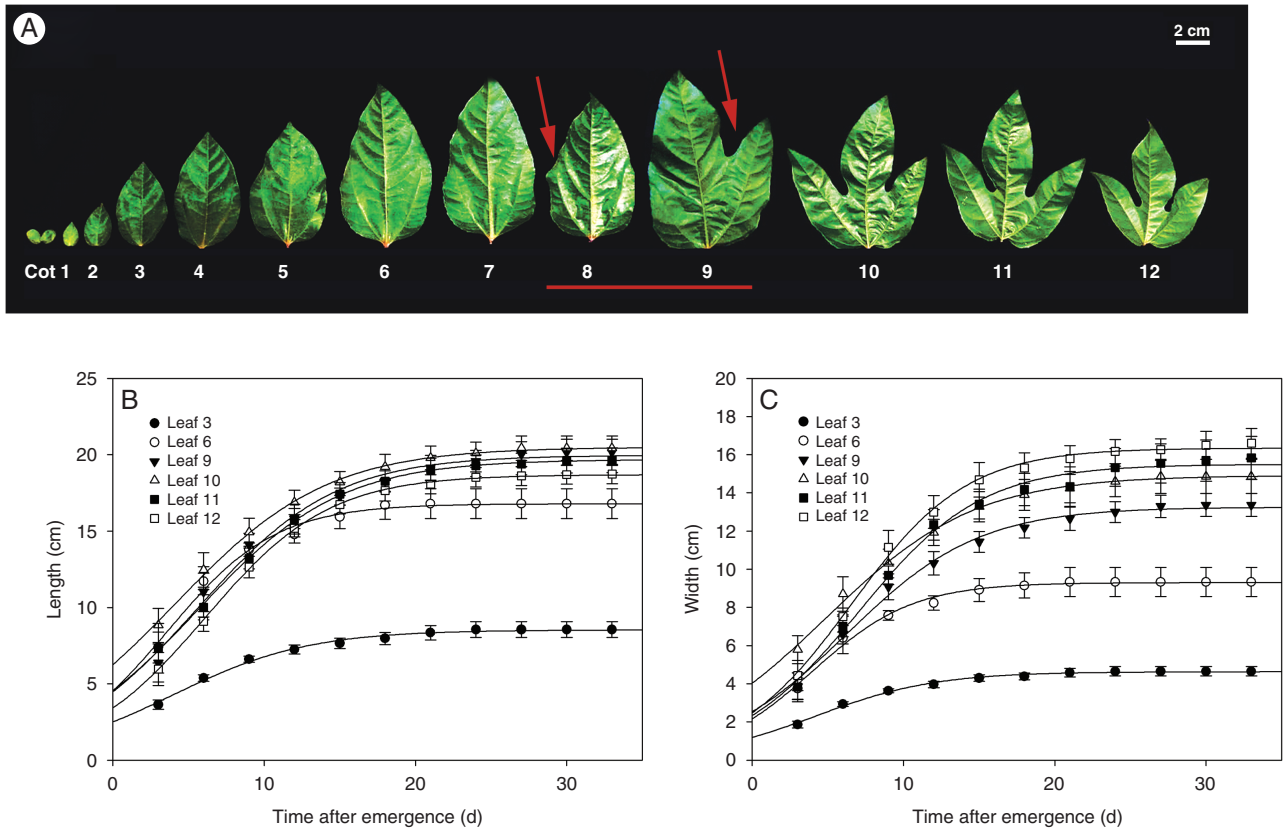

FIG. 1. Leaf morphology and growth dynamics during the heteroblastic process in *P. edulis*. (A) Overview of heteroblastic process during the time-course of leaf development from juvenile to adult in the vegetative phase. Left to right, from young monolobed to adult fully expanded trilobed leaves. Red line indicates leaves at intermediate stage, having both young and adult traits (red arrows). Cot, cotyledons. (B) Length and (C) width of the leaves were described by the sigmoidal function $y = A/(1 + \exp\{-[(x - x0)/b]\})$. Values are presented as mean ± s.e. of at least five individual determinations.

including heteroblasty (reviewed in Smeekens *et al.*, 2010; Yang *et al.*, 2013; Yu *et al.*, 2013; Buendía-Monreal and Gillmor, 2017). In *P. edulis*, sugar accumulation in leaf tissues correlated with the juvenile to adult phase transition (Fig. 3A). Throughout shoot development, glucose content increased substantially in adult leaves. Glucose levels increased from the ninth leaf onwards (Fig. 3A), which likely reflects an intermediate phase between vegetative transition from juvenile to adult (Fig. 1A). Fructose accumulation was similar to that of glucose, increasing gradually over the course of the vegetative phase change (Fig. 1A). Interestingly, fructose accumulation was 10-fold lower (2 µmol g^{-1}) than that of glucose (20 µmol g^{-1}). Sucrose levels, unlike those of glucose and fructose, presented only subtle variation during the vegetative phase change. Higher content of sucrose was observed in the third leaf, but the sucrose level declined slightly after the sixth leaf (Fig. 1A), perhaps because sucrose was broken down into glucose in the early steps of the glycolysis.

Overall metabolic responses vary according to the stage of organ ontogeny, and this variation may be crucial to the juvenile-to-adult transition (de Simón *et al.*, 2019). Therefore, we monitored the metabolic profile throughout leaf development of *P. edulis* (Fig. 3B). Data obtained were shown as a heat map (Fig. 3B) to facilitate the visualization of fluctuations in the levels of ~50 metabolites identified (most of them related to amino acids, organic acids and sugars). The original data are listed in Supplementary Data Table S2. The observed metabolite variation was most likely associated with the heteroblastic process, in which the young monolobed leaves undergo morphological changes to become adult trilobed ones (Fig. 1A). Hierarchical clustering based on the abundance of the identified metabolites was performed and revealed five well-distinguished clusters (Fig. 3B). The first cluster included metabolites such as succinate, malate, allo-inositol and glycerate, showing significant decreases in abundance in most leaf development stages when compared with the third leaf (reference sample). The second cluster was composed of threonine, leucine, acetoacate and isoleucine. These showed a slight increase in abundance in the three first leaves evaluated. The third cluster was characterized by metabolites with decreased abundance from the tenth leaf onwards. Isocaproic acid, methionine, ribulose, threonate and 2-oxoglutarate were the major metabolites of this cluster. Interestingly, the abundance of these metabolites decreased as the leaf acquired a complete trilobed morphological structure (Figs 1A and 3B). Intermediate organic acids from the second half of the tricarboxylic acid cycle, such as 2-oxoglutarate, succinate, fumarate, malate and oxaloacetate, showed either reduced abundance or did not significantly change throughout leaf morphological modifications (Fig. 3B). The fourth and fifth clusters were composed mainly of sugar-related metabolites. While the levels of metabolites grouped in the fourth cluster showed little change over the course of leaf development, the

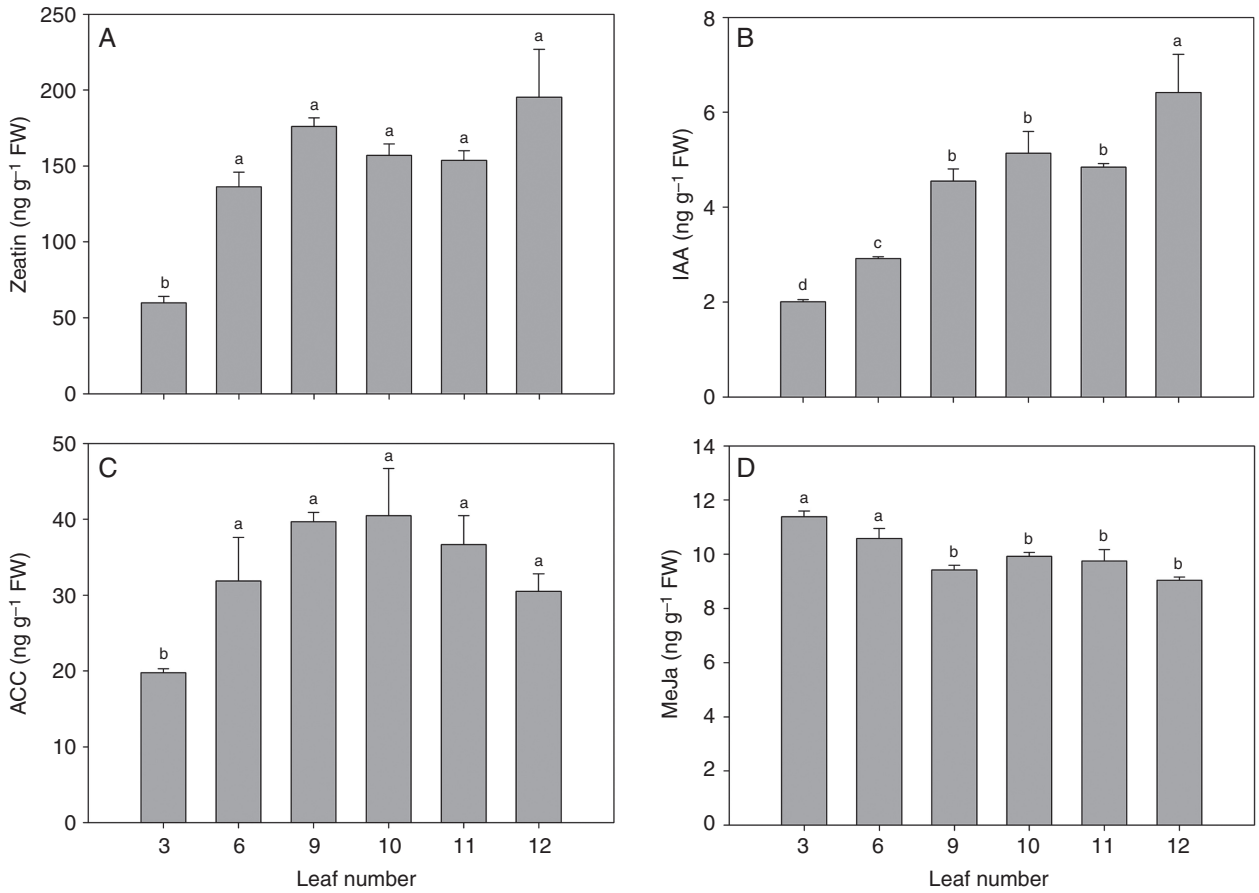

FIG. 2. Hormone levels change dynamically during the heteroblastic process in *P. edulis* leaves. Hormones were quantified at 30 dpe during leaf development from juvenile to adult. (A) Zeatin, (B) IAA, (C) ACC and (D) MeJa. Values are mean ± s.e. of five independent biological replicates. FW, fresh weight. Different lower-case letters indicate significant differences ($P < 0.05$).

fifth cluster showed the highest variation in metabolite abundance. The fifth cluster included glucose, fructose and sucrose, which showed similar accumulation patterns throughout leaf development, as detected by other techniques (Fig. 3A, B). It is worth mentioning that sorbose, rhamnose, myo-inositol-1-phosphate, raffinose, α-trehalose, glucoheptose, arabinose, isomaltose and phosphate-derived fructose (fructose-1-phosphate and fructose-6-phosphate) showed increasing abundance following juvenile-to-adult transition (Fig. 3B). Importantly, α-trehalose was one of the most induced metabolites during the heteroblastic process in leaves. Moreover, some amino acids, as well as their derivatives, were included in this cluster. Interestingly, the levels of the aromatic amino acid tryptophan increased from the third leaf onwards. This observation suggests that the increasing IAA levels observed during the progression of *P. edulis* leaf development (Fig. 2B) are likely due to the high abundance of tryptophan in adult leaves (Fig. 3B), since this amino acid is the major precursor of auxin.

To evaluate whether the observed metabolite changes are associated with the heteroblastic process or with the timing of development of *P. edulis* leaves, PCA was employed to compare the metabolic profiles between 15- and 30-dpe leaves (Supplementary Data Figure S1). In general, PCA revealed that the metabolic levels were more associated with the juvenile-to-adult phase transition than the timing of leaf development. For instance, metabolic profiles from 15- and 30-dpe leaves (Supplementary Data Tables S2 and S3) clustered together for the 11th and 12th leaves (Supplementary Data Fig. S1). The dispersion of each leaf in the first component (PC1 covered 52.9 % of the total variance) is explained mainly by changes in sugar levels (Supplementary Data Table S4), as already expected and shown in Fig. 3B. Sugars such as myo-insositol-1-phostate, alpha-trehalose and raffinose and tryptophan (an amino acid) are metabolites strongly correlated with the heteroblastic process in both 15- and 30-dpe leaves (Supplementary Data Table S4). Taken together, our findings suggest that the *P. edulis* heteroblastic process, instead of leaf age *per se*, is most likely governed by internal cues that trigger the observed metabolic changes. Thus, it seems that signalling events and metabolic changes may coordinate leaf morphological modifications associated with the heteroblastic process in this species.

Dynamic accumulation of miR156 and miR172 is associated with heteroblasty

We showed that sugar content increased as the *P. edulis* leaf aged (Fig. 3). Our results agree with the idea that sugars act as signalling molecules during leaf heteroblasty, perhaps via reducing miR156 accumulation, as they do in *Arabidopsis* (Yang *et al.*,

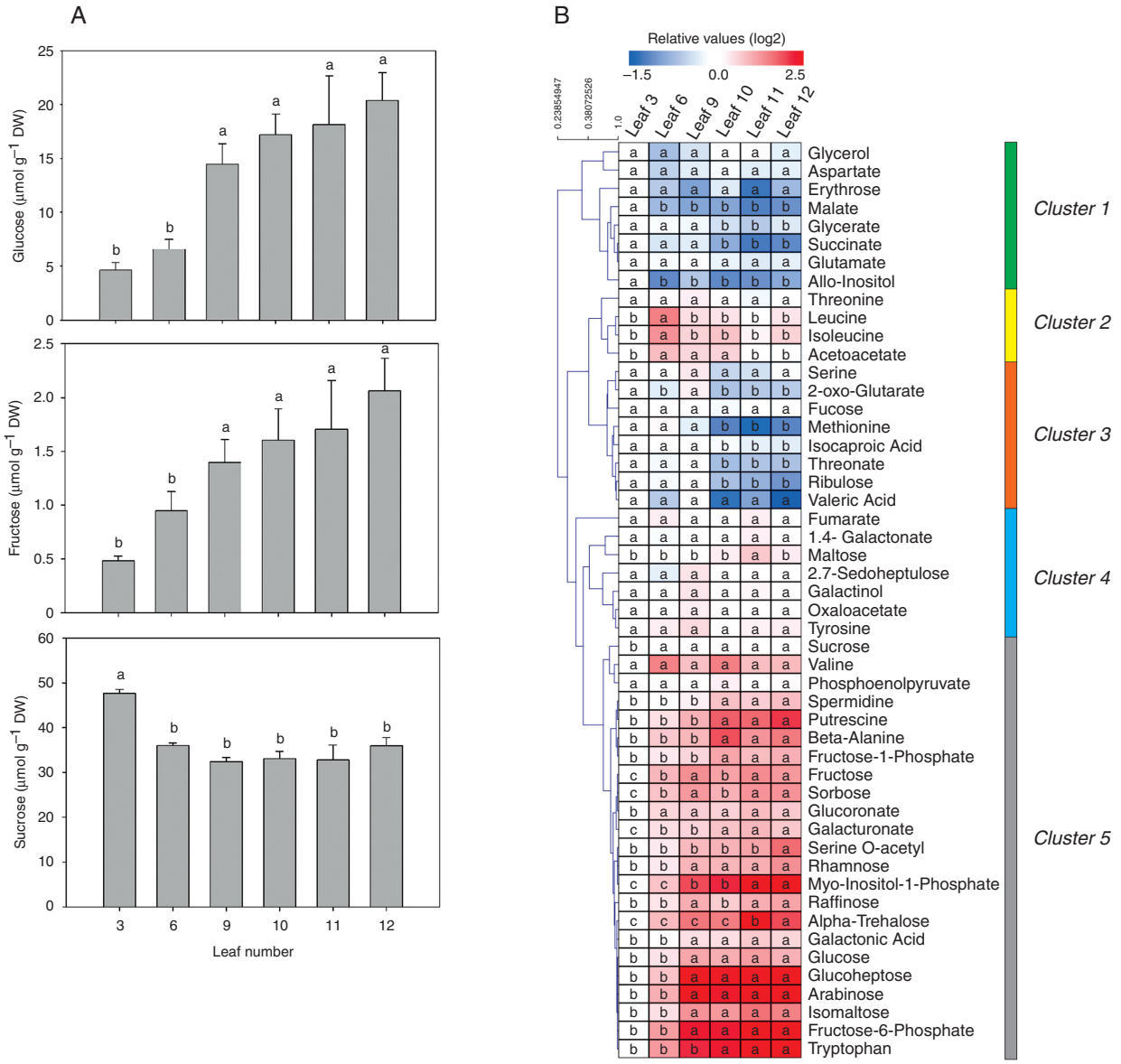

FIG. 3. Several metabolites, including soluble carbohydrates, dynamically change during the heteroblastic process in *P. edulis* leaves. (A) Glucose, fructose and sucrose were quantified during leaf development from juvenile to adult at 30 dpe. Values are mean ± s.e. of five independent biological replicates. Different lower-case letters indicate significant differences ($P < 0.05$). (B) Metabolite profiling of *P. edulis* leaf development was performed as described by Lisec *et al.* (2006). Data are presented as a heat map loaded with the mean of five independent biological replicates. Data were normalized with respect to the average response calculated for the third leaf. DW, dry weight. The colour code is given at $\log_2$ scale, in which blue and red represent down- and up-abundance, respectively. Different lower-case letters indicate significant differences ($P < 0.05$). The metabolites were grouped into five clusters, as described in the text.

2013; Yu *et al.*, 2013). We then monitored miR156 levels via stem–loop RT–qPCR during the heteroblastic process of *P. edulis* leaves (Fig. 4A). Mature miR156 transcript abundance was significantly reduced over the course of morphological changes in the leaves (Fig. 4A), thus showing an opposing accumulation pattern when compared with that of glucose and fructose (Fig. 3). On the other hand, miR172 expression levels were much higher in adult leaves (Fig. 4C). In *Arabidopsis*, miR156 and miR172 have opposing expression patterns during floral transition. During the transition to the reproductive phase miR156 levels decreased, allowing the expression of *MIR172b* (Wang *et al.*, 2009). Higher levels of miR172 lead to lower activity of its targets (the flowering repressor *AP2-like* genes; Yu *et al.*, 2015), allowing floral transition and flower development to take place. During *P. edulis* leaf development, miR172 transcript levels significantly increased from the sixth leaf onwards, an opposite expression pattern compared with that of miR156 (Fig. 4C). These observations suggest that miR156 and miR172 may have opposing roles associated with the heteroblastic process in this species. Interestingly, the variation in miR156 and miR172 transcript levels occurred earlier than the visible morphological switch from monolobed to trilobed shape in leaves (Figs 1A and 3A).

Another key component in the control of the juvenile-to-adult transition in *Arabidopsis* (Wang *et al.*, 2009), the

miR156-targeted *SPL9*, was characterized in *P. edulis*. The full-length *PeSPL9* mRNA (accession number MK142238) was 1534 bp in size, whereas the open reading frame (ORF) was 1110 bp in size, encoding a protein of 339 amino acids. The comparison of the *PeSPL9* protein sequence with other species available in NCBI and TAIR revealed similarity of 72, 65, 60, 60 and 43 % with *Ricinus communis*, *Vitis vinifera*, *Eucalyptus grandis*, *Citrus sinensis* and *A. thaliana*, respectively. The degree of sequence conservation, the presence of the SBP domain and the miR156 binding target site were all observed in the multiple sequence alignment analysis (Supplementary Data Fig. S1). The SBP domain (Cardon *et al.*, 1999) in PeSPL9 encompassed ~80 amino acid residues, with the presence of two zinc-finger binding sites: Zn1 with Cys-Cys-His-Cys, and another conserved Zn2, Cys-Cys-Cys-His (Supplementary Data Fig. S2A). The construction of a phylogenetic tree, supported by bootstrap values >50 %, showed that *PeSPL9* was grouped with species such as *Jatropha curcas*, *Manihot esculenta*, *R. communis* (members of the family Euphorbiaceae) and *Populus euphratica* (a member of the Salicaceae family). All of them, including *P. edulis*, belong to the order Malpighiales (Supplementary Data Fig. S2B). We observed a slight increase in *PeSPL9* transcript levels in adult leaves (Fig. 4B), opposite to the expression pattern observed for miR156 (Fig. 4A). However, it is possible that other *PeSPL*s may have a more prominent role in the heteroblastic process in *P. edulis* leaves.

Adult traits in leaves of P. edulis *are induced by glucose during* de novo *organogenesis*

Supplying *Arabidopsis* plants with exogenous glucose or fructose leads to the repression of miR156 accumulation and a concomitant increase in the proportion of leaves with morphological adult traits (Yang *et al.*, 2013). To better substantiate the correlation between the increasing levels of glucose and the heteroblastic process in *P. edulis* leaves (Fig. 3), we developed an assay to evaluate the role of glucose as a promoter of adult traits in *P. edulis* leaves during *de novo* organogenesis from cotyledonary explants. In this assay, we were able to synchronize leaf development and monitor the presence of the most obvious adult traits (i.e. serrations and lobules) in the leaves after supplementing the medium with glucose. We used inducing MS-based medium (IM) with half the hormone concentration used by Drew (1991) with or without glucose to ascertain that glucose is responsible for inducing adult characteristics *in vitro*. All culture media were able to induce *de novo* organogenesis of shoots and/or leaves (Table 1, Fig. 5). Trilobed leaves were observed in IM supplemented with 44 or 88 mM glucose (Fig. 5A, D, E), but not in IM lacking glucose (Fig. 5B, Table 1). We also observed leaves at intermediate stages of development when explants were cultured in treatments with glucose, in which juvenile-to-adult transition markers (lobules) were evident (Fig. 5C). These results suggested that glucose is involved in the heteroblastic process during *de novo* shoot organogenesis (Fig. 5), and that glucose may act similarly in the *ex vitro* heteroblastic process of *P. edulis* leaves (Figs 1A and 3). Therefore, our *in vitro* assay may be an interesting approach for future studies aiming to unravel the mechanisms underlying juvenile-to-adult phase transition in *P. edulis* leaves.

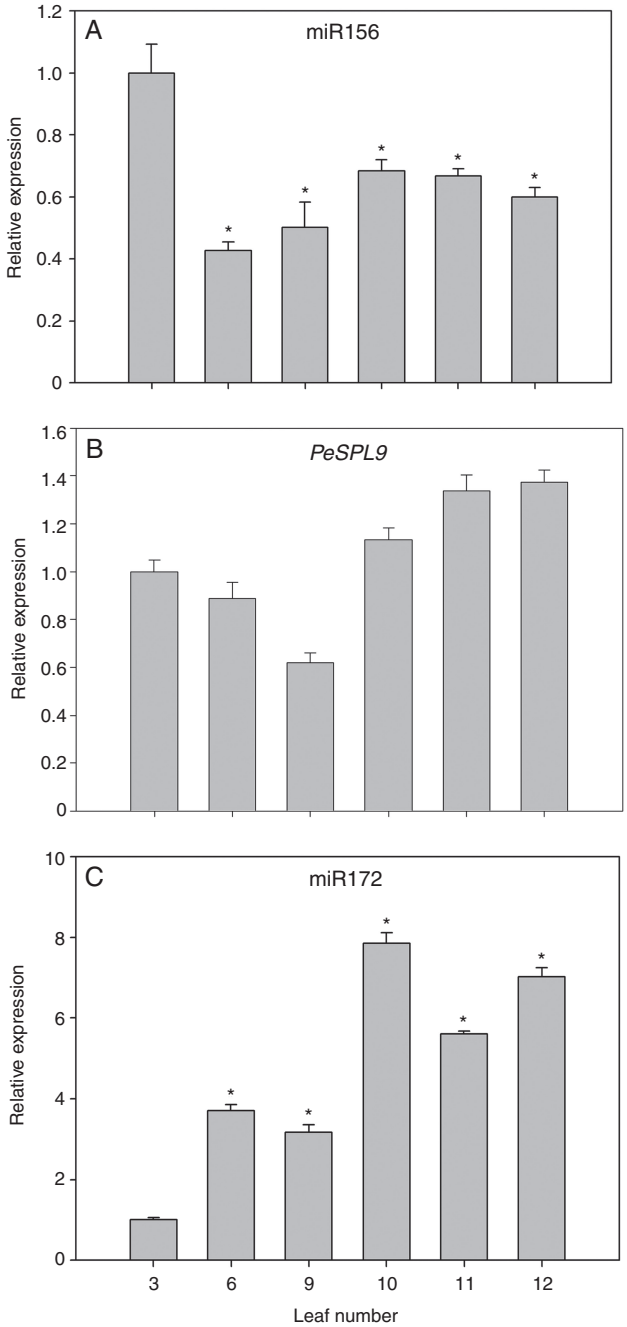

FIG. 4. Expression patterns of microRNAs and miR156-targeted *SPL9* during the heteroblastic process in *P. edulis* leaves. Relative expression at 30 dpe of (A) miR156, (B) *P. edulis SPL9* (*PeSPL9*) and (C) miR172 during leaf development. Values are mean ± s.e. of three independent biological replicates. Asterisks indicate significant differences ($P < 0.05$) between the third leaf and all other leaves.

Cotyledonary explants were collected 3 and 12 d after induction of *de novo* leaf organogenesis to monitor the expression levels of miR156 and *PeSPL9*. Interestingly, miR156 expression did not significantly change after glucose treatment at any time point (Fig. 5F). On the other hand, *PeSPL9* transcript levels increased at 3 d of culture in IM supplemented with both 44 and 88 mM of glucose (Fig. 5G). Our observations suggest that

the transcriptional levels of *PeSPL9* were positively regulated by glucose, likely independently of miR156.

PeSPL9 *is expressed in leaf primordia during* de novo *shoot organogenesis*

To determine the spatiotemporal expression pattern of *PeSPL9* during *de novo* organogenesis, we performed *in situ* hybridization to detect *PeSPL9* transcripts in stem buds and leaf shoots. Neoformation of meristemoids at different stages of development was evidenced 15 d after induction (Fig. 6A), with subsequent development of stem buds (Fig. 6B). Epidermal and cortical cells in dedifferentiation with subsequent formation of meristemoids showed the presence of *PeSPL9* transcripts (Fig. 6C). The control probe developed no hybridization signals (Supplementary Data Fig. S3), which confirmed the specificity of the observed expression patterns. In the subepidermal regions, where the processes of cellular dedifferentiation and meristemoid formation were not observed, *PeSPL9* transcripts were not detected (Fig. 6C, red arrowhead). In stem buds and leaf primordia developed from meristemoids, *PeSPL9* transcripts were detected (Fig. 6D, E). Interestingly, in the expanding leaf primordia there was a strong signal of *PeSPL9* transcripts, especially in epidermal cells of the abaxial leaf blade (Fig. 6F). These results indicate that *PeSPL9* was expressed early in the shoot apical meristem and leaf primordia and may participate in the heteroblastic process of leaf development.

DISCUSSION

The heteroblastic process of leaves from most *Passiflora* species clearly shows a transition from the juvenile to the adult phase (Cutri *et al.*, 2013). Heteroblastic modifications, which occur throughout leaf development, are mostly species-specific and are used as markers for species identification (Plotze *et al.*, 2005; Chitwood and Otoni, 2017*b*). In this work, we show that the heteroblastic patterns are drastically altered in *P. edulis* from the tenth leaf onwards (shootwards), going from monolobed to trilobed leaves (Cutri *et al.*, 2013; Fig. 1A). However, metabolite levels and the expression of microRNAs and targets changed earlier during heteroblastic development.

Our results showed that both juvenile and adult *P. edulis* leaf blades grew exponentially in length and width until ~15 dpe (Fig. 1B, C), similarly to other species of the *Passiflora* genus (Chitwood and Otoni, 2017*b*). During the progression of the heteroblastic process, zeatin and IAA levels increased in *P. edulis* leaves (Fig. 2). Both cytokinin and auxin can trigger alterations in leaf morphology (Efroni *et al.*, 2010; Byrne, 2012). For instance, high auxin concentration leads to the activation of *COTYLEDON CUP-SHAPED2* (*CUC2*), which in turn establishes adult patterns in *Arabidopsis* leaves (Bilsborough *et al.*, 2011; Byrne, 2012; Dkhar and Pareek, 2014). Moreover, increasing expression of *YUCCA* genes (which have a pivotal role in the tryptophan-dependent auxin biosynthesis pathway; Hentrich *et al.*, 2013) is correlated with increases in age and leaf complexity of the tree *Gevuina avellane* (Ostria-Gallardo *et al.*, 2016). Cytokinins, such as zeatin, are important for leaf development, promoting morphogenesis during juvenile-to-adult transition (Shwartz *et al.*, 2016). The effect of the cytokinin on leaf morphogenesis may be a result of its interaction with *KNOTTED1-LIKE HOMEOBOX* (*KNOX1*), as both are required for the regulation of leaf shape (Shani *et al.*, 2009; Uchida *et al.*, 2010; Bar and Ori, 2014).

Compelling evidence in *Arabidopsis* has indicated the pivotal role of microRNA-controlled modules in regulating leaf heteroblasty (Wu *et al.*, 2009; Yu *et al.*, 2015; Fouracre and Poethig, 2016). The miR156–*SPL* module is required for adult leaf transition (Huijser and Schmid, 2011; Jung *et al.*, 2011; Xu *et al.*, 2016). Our results showed that miR156 levels decreased throughout *P. edulis* leaf development, whereas *PeSPL9* transcript levels slightly increased in adult leaves (Fig. 4). Similar observations have been reported for *Arabidopsis* (Xu *et al.*, 2016). Despite the low variation in *SPL9* expression levels during leaf development, functional analyses in *Arabidopsis* have shown that miR156-targeted *SPL9* plays a dominant role in the expression of adult characteristics as well as flowering induction through transcriptional activation or repression (Usami *et al.*, 2009; Wu *et al.*, 2009; Jung *et al.*, 2011; Yu *et al.*, 2015; Xu *et al.*, 2016). In addition, SPL9 acts as a timing cue that destabilizes TEOSINTE BRANCHED 1/CYCLOIDEA/PCF (TCP)-CUC2 protein interactions during age-dependent leaf development in *Arabidopsis* and in the *Arabidopsis* relative *Cardamine hirsute* (Rubio-Somoza *et al.*, 2014). *Arabidopsis* SPL9 is also able to directly bind to the promoter of the *MIR172b* gene and increase miR172 transcript levels (Wu *et al.*, 2009). The role of miR172 in the vegetative-to-reproductive phase is well established, but its function in the heteroblastic process is less understood. In *P. edulis*, miR172 transcript levels were much higher in adult leaves (tenth to twelfth leaves), coinciding with the increase in *PeSPL9* transcript levels (Fig. 4). It is possible that *PeSPL9*-dependent regulation of miR172 accumulation may be an important mechanism during the heteroblastic process in *P. edulis*.

In addition to microRNA modules, metabolites also have a key role in triggering morphological changes during the transition from juvenile to adult leaves. Previous studies have reported the importance of primary metabolites in vegetative development (Corbesier *et al.*, 1998; Smeekens *et al.*, 2010). In general, sugar accumulation in *P. edulis* leaf tissues was correlated with juvenile-to-adult vegetative phase change (Fig. 3). This is in agreement with the fact that treating plants with sugar stimulates a substantial reduction in the abundance of miR156, suggesting that sugars may be a conserved 'timing' modulator of the miR156–*SPL* pathway (Yu *et al.*, 2013). Furthermore, analyses of loss-of-function mutants for photosynthesis have shown that photoassimilates are involved in the heteroblastic process (Tsai *et al.*, 1997; Yang *et al.*, 2013).

Our data also suggest the involvement of glucose in modulating adult leaf traits during *de novo* organogenesis in *P. edulis* (Fig. 5). Several studies have demonstrated the effect of soluble sugars in heteroblastic development in tissue culture (Allsopp, 1953; Sussex and Clutter, 1960; Feldman and Cutter, 1970). For instance, Allsopp (1953) demonstrated that *Marsilea drummondii* plants growing in the absence of an exogenous sugar source produced only young leaves, while medium supplemented with sugars accelerated the production of adult leaves. Glucose supplementation in IM led to the regeneration of *P. edulis* leaves with adult traits, with a consequent increase in

TABLE 1. *Role of glucose in the induction of the heteroblastic process in leaves of* P. edulis *during* de novo *organogenesis*

Treatment	Shoots (%)		Monolobed leaves (%)		Trilobed leaves (%)	
IM	36 ± 5	b	10 ± 4	b	0 ± 0.0	b
IM + 44 mM glucose	70 ± 3	a	58 ± 8	a	24 ± 4	a
IM + 88 mM glucose	84 ± 5	a	72 ± 4	a	16 ± 5	a

Values are mean ± s.e. of at least ten independent biological replicates. Different lower-case letters represent significant differences ($P < 0.05$) by the Scott–Knott test.

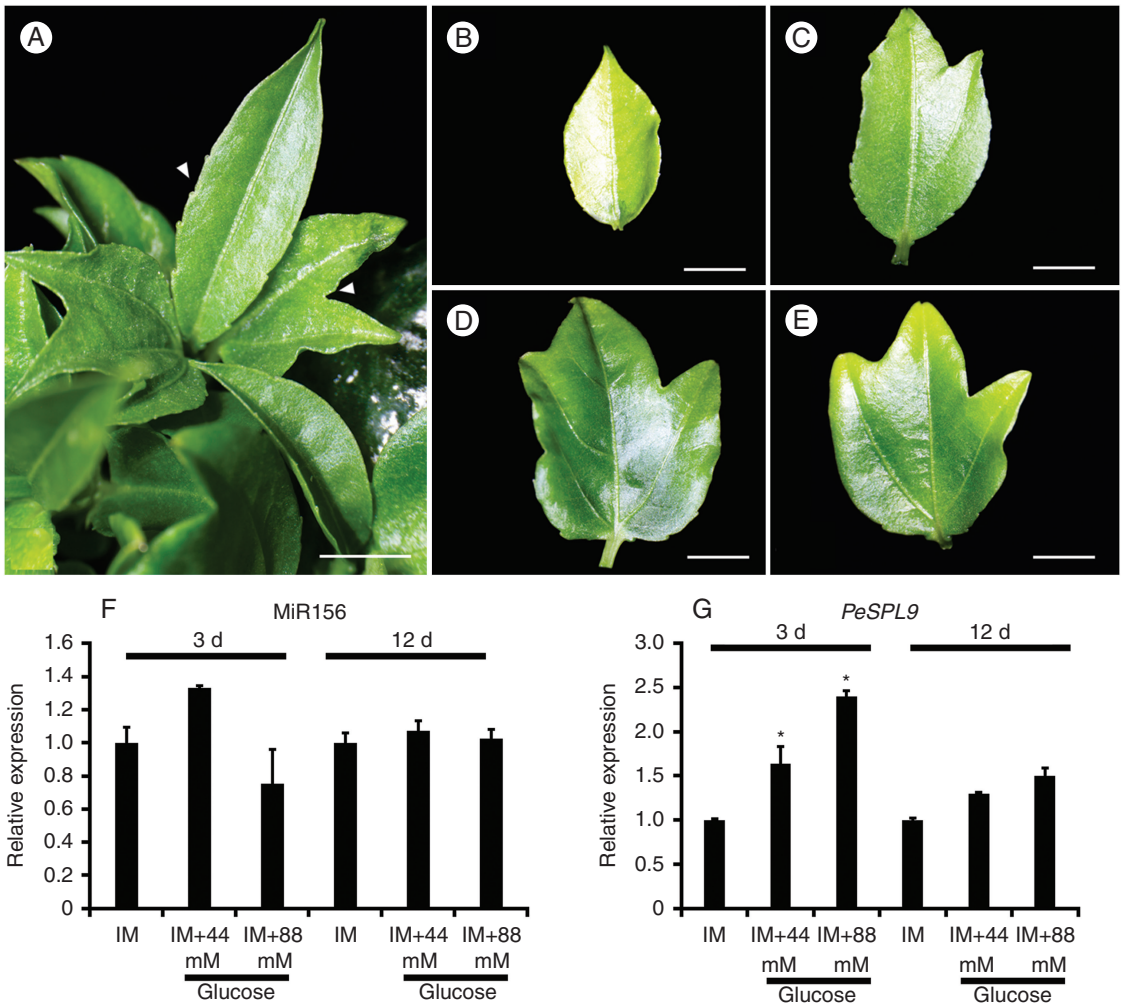

FIG. 5. *De novo* shoot and leaf organogenesis in *P. edulis* displays visible juvenile-to-adult leaf transition under glucose treatment. (A) Leaves showing adult traits of serration of the margin and lobe formation (arrowheads) when cotyledons were cultured on glucose-supplemented medium. (B) Young leaf with monolobed blade. (C, D) Leaves in intermediate stage of development, in which both types of juvenile–adult markers are present in the same leaf. (E) Adult leaf (trilobed). Scale bar = 3 mm. (F, G) Expression patterns of (F) miR156 and (G) miR156-targeted *SPL9* (*PeSPL9*) during *de novo* shoot and leaf organogenesis. Explants were cultivated in induction medium (IM) with or without 44 or 88 mM glucose for 3 or 12 d. Values are mean ± s.e. of at least two independent biological replicates. Asterisks indicate significant differences among treatments ($P < 0.05$).

PeSPL9 transcript levels (Fig. 5). These findings are consistent with previous studies in which glucose treatment led to the early appearance of adult traits in leaves via the regulation of miR156-targeted *SPL* expression (Yang *et al.*, 2013; Yu *et al.*, 2013, 2015).

Not only glucose but also other sugars might be associated with the heteroblastic process and phase changes throughout the plant life cycle (Proveniers, 2013; Wingler, 2018). We found that α-trehalose, arabinose and fructose-6-phosphate were the most abundant metabolites associated with the appearance of adult characters in 30-dpe *P. edulis* leaves (Fig. 3B). Trehalose is a signalling molecule involved in various developmental processes, such as senescence and flowering (Tsai and Gazzarrini, 2014; Figueroa and Lunn, 2016). In addition, trehalose-6-phosphate regulates the miR156–*SPL* module, promoting flowering in *Arabidopsis* (Wahl *et al.*, 2013). Sucrose levels changed

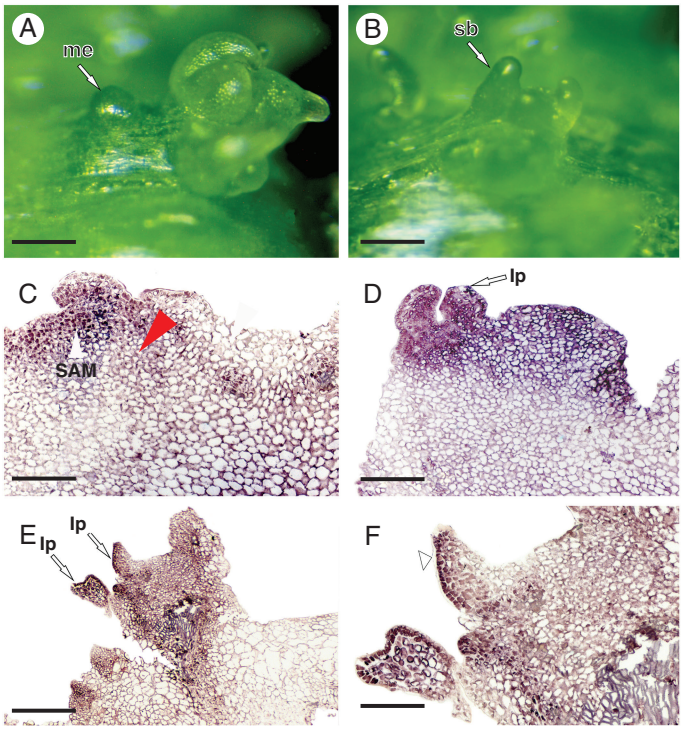

FIG. 6. *In situ* hybridization reveals that *SPL9* is expressed early during *de novo* shoot organogenesis in *P. edulis*. (A, B) Morphological characterization of the initiation of meristemoid formation followed by stem bud development. Stereomicroscope images. (C–F) Light microscope images. (C) Histological sections of the initiation of meristemoid formation highlighting *SPL9* gene expression in epidermal and parenchyma cells during the dedifferentiation process. (D, E) Detection of *PeSPL9* transcripts in the shoot apical meristem region and at leaf primordia initiation. (F) *PeSPL9* transcripts detected in epidermal cells of the abaxial surface of the leaf blade (arrowhead). Abbreviations: me, meristemoid; sb, stem bud; SAM, shoot apical meristem; lp, leaf primordium. Scale bars: (A, B) = 200 µm; (C, D, F) = 150 µm; (E) = 400 µm.

only slightly in adult leaves (Fig. 3A), suggesting that *P. edulis* may have other sugars promptly available or at least preferentially exported to other sink tissues. This role may be fulfilled in *P. edulis* leaves by raffinose, which accumulates in a profile similar to glucose and fructose (Fig. 3B), and it is considered a storage soluble sugar that is translocated throughout the plant (Van den Ende, 2013). In addition, myo-inositol-1-phosphate, a precursor in the synthesis of raffinose (Peterbauer and Richter, 2001), accumulated in trilobed leaves (Fig. 3B), suggesting that part of the raffinose biosynthesis pathway may also be associated with the heteroblastic process in *P. edulis* leaves.

How metabolic and genetic pathways interact to modulate age-dependent leaf shape establishment is more complex than previous anticipated. Thus, studies in non-model plants or in plants that do not have the genome completely sequenced are fundamental for the identification of molecular mechanisms involved in the heteroblastic process. In this work, we shed some light on the different molecular players associated with juvenile-to-adult leaf transition in a non-model species. Importantly, our data paved the way to future functional work on the miR156–*PeSPL9*–miR172 pathway in *P. edulis* and provide new metabolite candidates (e.g. α-trehalose and raffinose) that might be considered in further studies aiming to unravel the heteroblastic process in leaves.

SUPPLEMENTARY DATA

Supplementary data are available online at https://academic.oup.com/aob and consist of the following. Figure S1: PCA comparing metabolic profiles of 15- and 30-dpe leaves. Figure S2: characterization of *P. edulis* squamosa promoter binding protein-like 9 (PeSPL9). Figure S3: control sense *PeSPL9* probe used in the *in situ* hybridization assay. Table S1: list of primers used. Table S2: metabolite profiling of 30-dpe leaves of *P. edulis*. Table S3: relative metabolite content of 15- and 30-dpe leaves of *P. edulis* during the heteroblastic process. Table S4: PCA values based on metabolic data of *P. edulis* at 15 and 30 dpe.

ACKNOWLEDGEMENTS

We are grateful to Viveiro Flora Brasil (Araguari, Minas Gerais, Brazil) for providing the high-quality *P. edulis* seeds. We thank the Biomolecules Analysis Core (NUBIOMOL) at the Universidade Federal de Viçosa for providing facilities allowing hormonal and metabolomic analyses. The authors declare there is no conflict of interest. P.O.S., F.T.S.N. and W.C.O designed the research; P.O.S performed most of the research; D.B.S., J.H.F.C, A.D.K, L.V.M. and A.M.F. contributed new reagents/analytical tools; P.O.S., D.M.R., F.T.S.N. and W.C.O analysed the data; P.O.S., J.H.F.C, F.T.S.N. and W.C.O wrote the article with input from all the other authors. The Brazilian agencies Fundação de Amparo à Pesquisa do Estado de Minas Gerais (FAPEMIG, Belo Horizonte, MG, Brazil; grant CBB-APQ-01131-15) and Conselho Nacional de Desenvolvimento Científico e Tecnológico (CNPq, Brasília, DF, Brazil: grant 459.529/2014–5) are acknowledged for their support of W.C.O.

Research fellowships were granted by CNPq to F.T.S.N. and W.C.O. P.O.S. was recipient of a PhD scholarship from Coordenação de Aperfeiçoamento de Pessoal de Nível Superior (CAPES, Brasília, DF, Brazil). A.M.F. is currently a recipient of a Master scholarship from CAPES. D.S.B., J.H.F.C. and L.M.V. are currently recipients of post-doctoral scholarships from FAPEMIG (grant CBB-BPD-00020-16), FAPEMIG (grant CBB-BDP-00018-16) and CAPES/PNPD, respectively.

LITERATURE CITED

Allsopp A. 1953. Experimental and analytical studies of pteridophytes: XXI. Investigations on *Marsilea*. *Annals of Botany* **17**: 447–463.

Altschul SF, Madden TL, Schaffer AA, *et al.* 1997. Gapped BLAST and PSI-BLAST: a new generation of protein database search programs. *Nucleic Acids Research* **25**: 3389–3402.

Axtell MJ, Westholm JO, Lai EC. 2011. Vive la difference: biogenesis and evolution of microRNAs in plants and animals. *Genome Biology* **12**: 221.

Bar M, Ori N. 2014. Leaf development and morphogenesis. *Development* **141**: 4219–4230.

Bilsborough GD, Runions A, Barkoulas M, *et al.* 2011. Model for the regulation of *Arabidopsis thaliana* leaf margin development. *Proceedings of the National Academy of Sciences of the USA* **108**: 3424–3429.

Buendía-Monreal M, Gillmor CS. 2017. Convergent repression of miR156 by sugar and the CDK8 module of *Arabidopsis* Mediator. *Development Biology* **423**: 19–23.

Byrne ME. 2012. Making leaves. *Current Opinion in Plant Biology* **15**: 24–30.

Cardon G, Hohmann S, Klein J, Nettesheim K, Saedler H, Huijser P. 1999. Molecular characterisation of the *Arabidopsis* SBP-box genes. *Gene* **237**: 91–104.

Chen X, Zhang Z, Liu D, Zhang K, Li A, Mao L. 2010. *SQUAMOSA* promoter-binding protein-like transcription factors: star players for plant growth and development. *Journal of Integrative Plant Biology* **52**: 946–951.

Chitwood DH, Otoni WC. 2017*a*. Morphometric analysis of *Passiflora* leaves: the relationship between landmarks of the vasculature and elliptical Fourier descriptors of the blade. *GigaScience* **6**: 1–13.

Chitwood DH, Otoni WC. 2017*b*. Divergent leaf shapes among *Passiflora* species arise from a shared juvenile morphology. *Plant Direct* **1**: 1–15.

Chitwood DH, Ranjan A, Kumar R, *et al.* 2014. Resolving distinct genetic regulators of tomato leaf shape within a heteroblastic and ontogenetic context. *Plant Cell* **26**: 3616–3629.

Chuck G, Cigan AM, Saeteurn K, Hake S. 2007. The heterochronic maize mutant *Corngrass1* results from overexpression of a tandem microRNA. *Nature Genetics* **39**: 544–549.

Corbesier L, Lejeune P, Bernier G. 1998. The role of carbohydrates in the induction of flowering in *Arabidopsis thaliana*: comparison between the wild type and a starchless mutant. *Planta* **206**: 131–137.

Cronquist A. 1988. *The evolution and classification of flowering plants*, 2nd edn. New York: New York Botanical Garden.

Cutri L, Dornelas MC. 2012. PASSIOMA: exploring expressed sequence tags during flower development in *Passiflora* spp. *Comparative Functional Genomics* **2012**: 510549.

Cutri L, Nave N, Ami MB, Chayut N, Samach A, Dornelas MC. 2013. Evolutionary, genetic, environmental and hormonal-induced plasticity in the fate of organs arising from axillary meristems in *Passiflora* spp. *Mechanisms of Development* **130**: 61–69.

Dkhar J, Pareek A. 2014. What determines a leaf's shape? *EvoDevo* **5**: 47.

Drew RA. 1991. *In vitro* culture of adult and juvenile bud explants of *Passiflora* species. *Plant Cell, Tissue and Organ Culture* **26**: 23–27.

Efroni I, Eshed Y, Lifschitz E. 2010. Morphogenesis of simple and compound leaves: a critical review. *Plant Cell* **22**: 1019–1032.

Van den Ende W. 2013. Multifunctional fructans and raffinose family oligosaccharides. *Frontiers in Plant Science* **4**: 247.

Feldman LJ, Cutter EG. 1970. Regulation of leaf form in *Centaurea solstitialis* L. I. Leaf development on whole plants in sterile culture. *Botanical Gazette* **131**: 31–39.

Fernie AR, Roscher A, Ratcliffe RG, Kruger NJ. 2001. Fructose 2,6-bisphosphate activates pyrophosphate: fructose-6-phosphate 1-phosphotransferase and increases triose phosphate to hexose phosphate cycling in heterotrophic cells. *Planta* **212**: 250–263.

Figueroa CM, Lunn JE. 2016. A tale of two sugars: trehalose 6-phosphate and sucrose. *Plant Physiology* **172**: 7–27.

Fouracre JP, Poethig RS. 2016. The role of small RNAs in vegetative shoot development. *Current Opinion in Plant Biology* **29**: 64–72.

Gamage HK. 2011. Phenotypic variation in heteroblastic woody species does not contribute to shade survival. *AoB Plants* **2011**: plr013.

Gamborg OL, Miller RA, Ojima K. 1968. Nutrient requirements of suspension cultures of soybean root cells. *Experimental Cell Research* **50**: 151–158.

Gillmor CW, Silva-Ortega CO, Willmann MR, Buendía-Monreal M, Poethig RS. 2014. The *Arabidopsis* mediator CDK8 module genes CCT (MED12) and GCT (MED13) are global regulators of developmental phase transitions. *Development* **141**: 4580–4589.

Hentrich M, Böttcher C, Düchting P, *et al.* 2013. The jasmonic acid signaling pathway is linked to auxin homeostasis through the modulation of YUCCA8 and YUCCA9 gene expression. *Plant Journal* **74**: 626–637.

Huang H, Liu B, Liu L, Song S. 2017. Jasmonate action in plant growth and development. *Journal of Experimental Botany* **68**: 1349–1359.

Huijser P, Schmid M. 2011. The control of developmental phase transitions in plants. *Development* **138**: 4117–4129.

Jones-Rhoades MW, Bartel DP, Bartel B. 2006. MicroRNAs and their regulatory roles in plants. *Annual Review of Plant Biology* **57**: 19–53.

Jung JH, Seo PJ, Kang SK, Park CM. 2011. miR172 signals are incorporated into the miR156 signaling pathway at the *SPL3/4/5* genes in *Arabidopsis* developmental transitions. *Plant Molecular Biology* **76**: 35–45.

Khraiwesh B, Arif MA, Seumel GI, *et al.* 2010. Transcriptional control of gene expression by microRNAs. *Cell* **140**: 111–122.

Krumsiek J, Bartel J, Theis FJ. 2016. Computational approaches for systems metabolomics. *Current Opinion Biotechnology* **39**:198–206.

Kumar R. 2014. Role of microRNAs in biotic and abiotic stress responses in crop plants. *Applied Biochemistry and Biotechnology* **174**: 93–115.

Lagos-Quintana M, Rauhut R, Lendeckel W, Tuschl T. 2001. Identification of novel genes coding for small expressed RNAs. *Science* **294**: 853–858.

Levy A, Szwerdszarf D, Abu-Abied M, *et al.* 2014. Profiling microRNAs in *Eucalyptus grandis* reveals no mutual relationship between alterations in miR156 and miR172 expression and adventitious root induction during development. *BMC Genomics* **15**: 524.

Lisec J, Schauer N, Kopka J, Willmitzer L, Fernie AR. 2006. Gas chromatography mass spectrometry-based metabolite profiling in plants. *Nature Protocols* **1**: 387–396.

Liu Q, Chen YQ. 2009. Insights into the mechanism of plant development: interactions of miRNAs pathway with phytohormone response. *Biochemical and Biophysical Research Communications* **384**: 1–5.

Livak KJ, Schmittgen TD. 2001. Analysis of relative gene expression data using real-time quantitative PCR and the $2^{-\text{Anal}}$ method. *Methods* **25**: 402–408.

Luedemann A, Strassburg K, Erban A, Kopka J. 2008. TagFinder for the quantitative analysis of gas chromatography–mass spectrometry (GC-MS)-based metabolite profiling experiments. *Bioinformatics* **24**: 732–737.

Mallory AC, Vaucheret H. 2006. Functions of microRNAs and related small RNAs in plants. *Nature Genetics Supplement* **38**: 31–36.

Morea-Ortiz EG, Silva EM, Silva GFF, *et al.* 2016. Functional and evolutionary analyses of the miR156 and miR529 families in land plants. *BMC Plant Biology* **16**: 40.

Murashige T, Skoog F. 1962. A revised medium for rapid growth and bio assays with tobacco tissue cultures. *Physiologia Plantarum* **15**: 473–497.

Napoleão TA, Soares G, Vital CE, *et al.* 2017. Methyl jasmonate and salicylic acid are able to modify cell wall but only salicylic acid alters biomass digestibility in the model grass *Brachypodium distachyon*. *Plant Science* **263**: 46–54.

Nave N, Katz E, Chayut N, Gazit S, Samach A. 2010. Flower development in the passion fruit *Passiflora edulis* requires a photoperiod-induced systemic graft-transmissible signal. *Plant, Cell & Environment* **33**: 2065–2083.

Nguyen STT, Greaves T, McCurdy DW. 2017. Heteroblastic development of transfer cells is controlled by the microRNA miR156/*SPL* module. *Plant Physiology* **173**: 1676–1691.

Ostria-Gallardo E, Ranjan A, Chitwood DH, *et al.* 2016. Transcriptomic analysis suggests a key role for SQUAMOSA PROMOTER BINDING PROTEIN LIKE, NAC and YUCCA genes in the heteroblastic development of the temperate rainforest tree *Gevuina avellana* (Proteaceae). *New Phytologist* **210**: 694–708.

Peterbauer T, Richter A. 2001. Biochemistry and physiology of raffinose family oligosaccharides and galactosyl cyclitols in seeds. *Seed Science Research* **11**: 185–197.

Plotze RDO, Falvo M, Pádua JG, *et al.* 2005. Leaf shape analysis using the multiscale Minkowski fractal dimension, a new morphometric method: a study with *Passiflora* (Passifloraceae). *Canadian Journal of Botany* **83**: 287–301.

Poethig RS. 2010. The past, present, and future of vegetative phase change. *American Society of Plant Biologists* **2**: 541–544.

Proveniers M. 2013. Sugars speed up the circle of life. *eLife* **2**: e00625.

Reis LB, Neto VBP, Picoli EAT, *et al.* 2003. Axillary bud development of passionfruit as affected by ethylene precursor and inhibitors. *In Vitro Cellular and Developmental Biology – Plant* **39**: 618–622.

Rocha DI, Vieira LM, Koelher AD, Otoni WC. 2018. Cellular and morpho-histological foundations of *in vitro* plant regeneration. In: Loyola-Vargas VM, Ochoa-Alejo N, eds. *Plant cell culture protocols. Methods in molecular biology*, Vol. **1815**, 4th edn. New York: Humana Press.

Roessner U, Luedemann A, Brust D, *et al.* 2001. Metabolic profiling and phenotyping of genetically and environmentally modified systems. *Plant Cell* **13**: 11–29.

Rubio-Somoza I, Zhou CM, Confraria A, *et al.* 2014. Temporal control of leaf complexity by miRNA-regulated licensing of protein complexes. *Current Biology* **24**: 2714–2719.

Saitou N, Nei M. 1987. The neighbour joining method: a new method for reconstructing phylogenetic trees. *Molecular Biology and Evolution* **4**: 406–425.

Scott RJ, Knott M. 1974. A cluster analysis method for grouping means in the analysis of variance. *Biometrics* **30**: 507–512.

Shani E, Burko Y, Ben-Yaakov L, Berger Y, *et al.* 2009. Stage-specific regulation of *Solanum lycopersicum* leaf maturation by class 1 KNOTTED1-LIKE HOMEOBOX proteins. *Plant Cell* **21**: 3078–3092.

Shwartz I, Levy M, Ori N, Bar M. 2016. Hormones in tomato leaf development. *Developmental Biology* **419**: 132–142.

Smeekens S, Ma J, Hanson J, Rolland F. 2010. Sugar signals and molecular networks controlling plant growth. *Current Opinion in Plant Biology* **13**: 274–279.

Silva GF, Silva EM, Correa JP, *et al.* 2019. Tomato floral induction and flower development are orchestrated by the interplay between gibberellin and two unrelated microRNA-controlled modules. *New Phytologist* **221**: 1328–1344.

de Simón BF, Cadahía E, Aranda I. 2019. Metabolic response to elevated CO_2 levels in *Pinus pinaster* Aiton needles in an ontogenetic and genotypic-dependent way. *Plant Physiology and Biochemistry* **132**: 202–212.

Sussex IM, Clutter ME. 1960. A study of the effect of externally supplied sucrose on the morphology of excised fern leaves *in vitro*. *Phytomorphology* **10**: 87–99.

Tsai AYL, Gazzarrini S. 2014. Trehalose-6-phosphate and SnRK1 kinases in plant development and signaling: the emerging picture. *Frontiers in Plant Science* **5**: 119.

Tsai CH, Miller A, Spalding M, Rodermel S. 1997. Source strength regulates an early phase transition of tobacco shoot morphogenesis. *Plant Physiology* **115**: 907–914.

Tsukaya H. 2013. Leaf development. *The Arabidopsis Book* **11**: e0163.

Uchida N, Kimura S, Koenig D, Sinha N. 2010. Coordination of leaf development via regulation of *KNOX1* genes. *Journal of Plant Research* **123**: 7–14.

Usami T, Horiguchi G, Yano S, Tsukaya H. 2009. The more and smaller cells mutants of *Arabidopsis thaliana* identify novel roles for *SQUAMOSA PROMOTER BINDING PROTEIN-LIKE* genes in the control of heteroblasty. *Development* **136**: 955–964.

Varkonyi-Gasic E, Wu R, Wood M, Walton EF, Hellens RP. 2007. Protocol: a highly sensitive RT-PCR method for detection and quantification of microRNAs. *Plant Methods* **3**: 1–12.

Wahl V, Ponnu J, Schlereth A, *et al.* 2013. Regulation of flowering by trehalose-6-phosphate signaling in *Arabidopsis thaliana*. *Science* **339**: 704–707.

Wang JW, Czech B, Weigel D. 2009. miR156-regulated *SPL* transcription factors define an endogenous flowering pathway in *Arabidopsis thaliana*. *Cell* **138**: 738–749.

Wang JW, Park MY, Wang LJ, *et al.* 2011. MiRNA control of vegetative phase change in trees. *PLoS Genetics* **7**: 1002012.

Wang L, Sun S, Jin J, *et al.* 2015. Coordinated regulation of vegetative and reproductive branching in rice. *Proceedings of the National Academy of Sciences of the USA* **112**: 15504–15509.

De Wilde WJJO. 1971. The systematic position of the tribe Paropsieae, in particular the genus *Ancistrothyrsus*, and a key to the genera of Passifloraceae. *Blumea* **19**: 99–104.

Wingler A. 2018. Transitioning to the next phase: the role of sugar signaling throughout the plant life cycle. *Plant Physiology* **176**: 1075–1084.

Wu G, Park MY, Conway SR, Wang J, Weigel D, Poethig RS. 2009. The sequential action of miR156 and miR172 regulates developmental timing in *Arabidopsis. Cell* **138**: 750–759.

Xu M, Hu T, Zhao J, *et al.* 2016. Developmental functions of miR156-Regulated *SQUAMOSA PROMOTER BINDING PROTEIN-LIKE (SPL)* genes in *Arabidopsis thaliana*. *PLoS Genetics* **12**: 1006263.

Xu M, Leichty AR, Hu T, Poethig RS. 2018. H2A.Z promotes the transcription of *MIR156A* and *MIR156C* in *Arabidopsis* by facilitating the deposition of H3K4me3. *Development* **145**: doi:10.1242/dev.152868.

Xu Y, Zhang L, Wu G. 2018. Epigenetic regulation of juvenile-to-adult transition in plants. *Frontiers in Plant Science* **17**: 1048.

Yang L, Conway SR, Poethig RS. 2011. Vegetative phase change is mediated by a leaf-derived signal that represses the transcription of miR156. *Development* **138**: 245–249.

Yang L, Xu M, Koo Y, He J, Poethig RS. 2013. Sugar promotes vegetative phase change in *Arabidopsis thaliana* by repressing the expression of *MIR156A* and *MIR156C*. *eLife* **2**: e00260.

Yu S, Cao L, Zhou CM, *et al.* 2013. Sugar is an endogenous cue for juvenile-to-adult phase transition in plants. *eLife* **2**: e00269.

Yu S, Lian H, Wang W. 2015. Plant developmental transitions: the role of microRNAs and sugars. *Current Opinion in Plant Biology* **27**: 1–7.